



Deposited via The University of Leeds.

White Rose Research Online URL for this paper:

<https://eprints.whiterose.ac.uk/id/eprint/96557/>

Version: Accepted Version

Article:

Moazen, M, Alazmani, A, Rafferty, K et al. (2016) Intracranial pressure changes during mouse development. *Journal of Biomechanics*, 49 (1). pp. 123-126. ISSN: 0021-9290

<https://doi.org/10.1016/j.jbiomech.2015.11.012>

© 2015, Elsevier. Licensed under the Creative Commons Attribution-NonCommercial-NoDerivatives 4.0 International <http://creativecommons.org/licenses/by-nc-nd/4.0/>

Reuse

Items deposited in White Rose Research Online are protected by copyright, with all rights reserved unless indicated otherwise. They may be downloaded and/or printed for private study, or other acts as permitted by national copyright laws. The publisher or other rights holders may allow further reproduction and re-use of the full text version. This is indicated by the licence information on the White Rose Research Online record for the item.

Takedown

If you consider content in White Rose Research Online to be in breach of UK law, please notify us by emailing eprints@whiterose.ac.uk including the URL of the record and the reason for the withdrawal request.

1 **Short communication**

2 **Intracranial pressure changes during mouse development**

3

4 **Mehran Moazen¹, Ali Alazmani², Katherine Rafferty³, Zi-Jun Liu³, Jennifer Gustafson⁴,**
5 **Michael L Cunningham⁴, Michael J Fagan⁵, Susan W Herring³**

6

7 ¹Department of Mechanical Engineering, University College London, Torrington Place,
8 London WC1E 7JE, UK

9 ²Institute of Functional Surfaces, School of Mechanical Engineering, University of Leeds,
10 Leeds, LS2 9JT, UK

11 ³Department of Orthodontics, University of Washington, Seattle, WA 98195-7446, USA

12 ⁴Seattle Children's Research Institute, Center for Developmental Biology & Regenerative
13 Medicine and Seattle Children's Craniofacial Center, Seattle, WA 98105, USA

14 ⁵Medical and Biological Engineering, School of Engineering, University of Hull, Hull, HU6
15 7RX, UK

16

17

18

19 Corresponding author:

20 Mehran Moazen, BSc, PhD, CEng, MIMechE, FHEA

21 Department of Mechanical Engineering,

22 University College London,

23 Torrington Place,

24 London WC1E 7JE, UK

25 Tel: +44 (0) 208 954 8056; Fax: +44 (0) 208 954 6371

26 Email: Mehran_Moazen@yahoo.com; M.Moazen@ucl.ac.uk

27

28 Word count (Introduction through Discussion): 2005

29

30

31

32

33

34

35 **Abstract:**

36 During early stages of postnatal development, pressure from the growing brain as well as
37 cerebrospinal fluid, i.e. intracranial pressure (ICP), load the calvarial bones. It is likely that
38 such loading contributes to the peripheral bone formation at the sutural edges of calvarial
39 bones, especially shortly after birth when the brain is growing rapidly. The aim of this study
40 was to quantify ICP during mouse development. A custom pressure monitoring system was
41 developed and calibrated. It was then used to measure ICP in a total of seventy three wild
42 type mice at postnatal (P) day 3, 10, 20, 31 and 70. Retrospectively, the sample in each age
43 group with the closest ICP to the average value was scanned using micro-computed
44 tomography to estimate cranial growth. ICP increased from 1.33 ± 0.87 mmHg at P3 to
45 1.92 ± 0.78 mmHg at P10 and 3.60 ± 1.08 mmHg at P20. In older animals, ICP plateaued at
46 about 4 mmHg. There were statistically significant differences between the ICP at the P3 vs.
47 P20, and P10 vs. P20. In the samples that were scanned, intracranial volume and skull
48 length followed a similar pattern of increase up to P20 and then plateaued at older ages.
49 These data are consistent with the possibility of ICP being a contributing factor to bone
50 formation at the sutures during early stages of development. The data can be further used
51 for development and validation of computational models of skull growth.

52

53 **Key words:** Intracranial pressure, Skull, Suture, Biomechanics, Development

54 **Introduction:**

55 During early stages of postnatal development, intracranial pressure (ICP), from the growing
56 brain and cerebrospinal fluid load calvarial bones and sutures (Moss, 1954; Cohen, 1993;
57 Opperman, 2000; Herring, 2008). It is likely that such loading contributes as an epigenetic
58 factor to the peripheral bone formation at the edges of calvarial bones just after birth. Once
59 forceful mastication starts, muscles also load the craniofacial system and presumably
60 influence cranial growth (Nakata, 1981; Rafferty and Herring, 1999; Al Dayeh et al., 2013).
61 While there is a large ongoing effort to understand the genetic causes of various craniofacial
62 developmental disorders (e.g. Morriss-Kay and Wilkie, 2005; Richtsmeier and Flaherty,
63 2013; Cox et al., 2013), understanding epigenetic factors such as biomechanical loading
64 based on ICP during normal and abnormal development is crucial too. A broad
65 understanding of the various factors involved in the development of the craniofacial system
66 can in the long term enhance the treatment of various congenital diseases such as
67 craniosynostosis and Treacher Collins syndrome.

68

69 Quantifying ICP in infants is clearly challenging, but animal models can provide invaluable
70 insights. In particular, accurate invasive but accurate methods can be employed, rather than
71 non-invasive methods that are safer for children but inadequate for this study (Silasi et al.,
72 2009; Raboel et al., 2012; Murtha et al., 2012; Uldall et al., 2014). Mice are particularly
73 useful in that like other mammals, they have many similarities to humans in terms of calvarial
74 morphology and genome (Morriss-Kay and Wilkie, 2005), their genetics is well characterized
75 and there are models available to investigate the pathogenesis of various craniofacial
76 deformities. Despite a long-standing interest in skull development in mice (e.g. Fong et al.,
77 2003; Henderson, et al., 2005) and rats (e.g. Jones et al., 1987), to the best of our
78 knowledge, intracranial pressure during normal mouse development has not been quantified
79 previously. Such data can be used to enhance our understanding of the biomechanics of
80 normal calvarial growth and possibly, ultimately, management of related congenital

81 diseases. Therefore, the aims of this study were to develop a suitable ICP measurement
82 system and quantify ICP during wild type mouse development. To highlight morphological
83 changes during development one sample per age group was scanned and analysed.

84

85 **Materials and Methods:**

86 A pressure monitoring system was developed to measure ICP in mice of 5 age groups. ICP
87 was recorded while animals were anaesthetised. Following the recording animals were
88 decapitated while still under anaesthesia. Then, the sample with closest ICP to the average
89 ICP for each age group was selected for morphological analysis.

90

91 **Pressure monitoring system:** A 22-gauge needle (outer diameter 0.70 mm; length 6 mm)
92 was connected via luer-lock to silicone tubing (outer diameter 4 mm; length 250 mm) which
93 was then connected to a differential pressure sensor (TruStability® Board Mount Pressure
94 Sensors: HSC Series, Honeywell, NJ, USA). The measurement range of the sensor was
95 ± 18.68 mmHg with total error band of 0.19 mmHg. The signal, i.e. changes in the voltage
96 due to external pressure at the tip of the needle, was acquired at 100 Hz using a custom
97 program written in LabVIEW 2013 (National Instruments Corp, Austin, TX, USA). The
98 pressure measurement system was calibrated using tubes with 50, 70, 100, 120 and 150
99 mm of water, with each test repeated five times.

100

101 **In vivo recording of ICP:** A total of seventy-three inbred wild type mice (*Mus musculus*,
102 C57BL/6J - Jackson Labs, Bar Harbor, Maine, USA) at postnatal (P) day 3 (2.23 ± 0.27 g), 10
103 (5.05 ± 1.1 g), 20 (9.06 ± 1.48 g), 31 (17.75 ± 1.91 g) and 70 (22.46 ± 4.01 g) were used. Sex
104 was not recorded for the younger groups, but a retrospective statistical analysis comparing
105 the ICP between males and females at P31 did not show a significant difference. The P70
106 mice were all female. All protocols were approved by the Institutional Animal Care and Use
107 Committees of the University of Washington and Seattle Children's Research Institute. Mice

108 were anesthetized using isoflurane in a non-rebreathing custom set-up. During testing heat
109 support was provided via a warm water pad. Once the animals did not respond to toe pinch,
110 a sagittal incision was made over the calvaria. The needle was inserted through the left
111 parietal bone ca. 2 mm lateral to the sagittal suture and 2 mm anterior to the lambdoid
112 suture. With care it was possible to penetrate the bone with the needle even in older
113 animals, but it was important not to enlarge the hole beyond its diameter. The needle was
114 inserted to a depth calculated to position it in the subarachnoid space, which is filled with
115 cerebrospinal fluid. No external pressure was applied to the skull once the needle had been
116 inserted. It was held in place until ICP reached a maximum (typically 1-2 min); when ICP
117 began to drop, or after several minutes if it did not drop, the needle was removed and the
118 maximum recorded pressure was reported. Once recording was completed, the animals
119 were decapitated while still under anaesthesia.

120

121 **Statistical analysis:** Statistical analysis was performed in SPSS (IBM SPSS, NY, USA).
122 One-way analysis of variance (ANOVA) with post-hoc Bonferroni and Tukey tests was
123 carried out, with Levene's test used to test for equal variances. The significance level was
124 set at $p < 0.05$.

125

126 **Ex vivo micro-computed tomography:** The specimen with measured ICP closest to the
127 average ICP value of each age group was scanned using an X-Tek HMX 160 micro-CT
128 scanner (XTek Systems Ltd, Hertfordshire, UK) with a voxel size of 0.01mm in x, y, and z
129 directions. AVIZO (FEI Visualization Sciences Group, Merignac Cedex, France) was used to
130 reconstruct three dimensional models. The scans were automatically aligned with respect to
131 each other in AVIZO based on minimization of the root mean square distance between the
132 nodes forming the triangulated surfaces of the skull (i.e., Procrustes method) using an
133 iterative closest point algorithm. Each skull surface was typically consisted of about 300,000
134 nodes. Skull length, width and intracranial volume (ICV) were measured using the software.

135

136 **Results:**

137 **Sensor calibration:** As the needle was gradually moved down the tube of water, voltage
138 gradually increased, plateauing at the bottom of the tube. Similarly, upon removal from the
139 water, voltage decreased to its baseline value (Fig 1A). Calibration of the sensor at various
140 heights of water (each repeated five times) showed that the corresponding voltage changes
141 were stable, repeatable and linear (Fig 1B). Note the error bars corresponding to one
142 standard deviation (of five repeats) are shown in Fig 1B. These values were in the range of
143 0.004-0.01 V. These calibration data were used to convert the voltage changes during ICP
144 measurement to mmHg.

145

146 **ICP Measurements:** ICP was 1.33 ± 0.87 mmHg at P3, increasing to 1.92 ± 0.78 mmHg at
147 P10, 3.60 ± 1.08 mmHg at P20, 3.81 ± 1.14 mmHg at P31 and 4.11 ± 0.83 mmHg at P70.
148 There were statistically significant differences between P3 vs. P20, P31, P70, and P10 vs.
149 P20, P31, P70, but not between P20, P31 and P70 (Fig 2).

150

151 **Morphological changes:** Skull length was 13 mm in the P3 skull and 17, 19, 20 and 22 mm
152 at P10, P20, P31 and P70 respectively. Skull width increased to a lesser extent from 8 mm
153 at P3 to 11 mm at P70. ICV increased from 240 mm³ at P3 to 339, 462, 474 and 504 mm³ at
154 P10, P20, P31 and P70 respectively (Fig 3).

155

156 **Discussion:**

157 Intracranial pressure may be an important factor contributing to calvarial bone formation at
158 the cranial sutures during early postnatal stages of development. In this study ICP during
159 mouse development was quantified at several postnatal ages in a relatively large number of
160 specimens (10-20 at each age). These ages were chosen to capture various stages of
161 development from just after birth (P3) to juvenile (P10 and P20) to early adulthood (P30 and

162 P70 - see e.g. Hill et al., 2008; Flurkey et al., 2007). Notably, the majority of volumetric brain
163 growth in mice occurs by P20 with lesser increase during P30-P80 (e.g. Zhang et al., 2005).
164 Despite the initial calibration test and repeatability of the results, it is important to compare
165 the ICP data with the existing literature. While no data exist on ICP during mouse
166 development, several studies have quantified ICP in adult mice. Oshio et al. (2004) reported
167 ICP of 6.99 ± 1.03 mmHg in the lateral ventricle (P56-70; n=6), Feiler et al. (2010) reported
168 ICP of 5.0 ± 0.5 mmHg in the epidural space (body weight 23-25 g; n=6), and Yang et al.
169 (2008) reported ICP of 4.33 ± 0.62 mmHg (P70; n=7). Our location, chosen to correspond
170 with our ongoing biomechanical studies on the frontoparietal region (e.g. Moazen et al.,
171 2015), is close to that examined by Yang et al. (2008) i.e. 1 mm posterior to the coronal
172 suture and 1 mm lateral to the sagittal suture. ICP recorded for P70 mice in this study was
173 4.11 ± 0.83 mmHg (n=13), well within the range of data reported by Yang et al. (2008). This is
174 reassuring, as it validates the ability of our sensor to produce reasonable and reliable data
175 for the younger ages in the present study.

176

177 The data obtained showed that ICP increases from about 1.3 mmHg in P3 to 3.6 mmHg in
178 P20 to a limit of approximately 4 mmHg in mice older than P20. This finding is similar to that
179 of Mooney et al. (1998) who measured epidural ICP during rabbit development and reported
180 an increase in ICP from 3.24 ± 0.36 mmHg at P25 (n=28) to 5.68 ± 0.38 mmHg at P42 (n=21).
181 Our morphological measurements are also in agreement with literature (e.g. Zhang et al.,
182 2005; Aggarwal et al., 2009; Chuang et al., 2011). For example, our ICVs of 240, 461 and
183 504 mm^3 at P3, P20 and P70 are comparable to the values of 200, 400 and 430 mm^3
184 reported by Chuang et al. (2011) in C57BL/6 mice at the same ages.

185

186 ICP, ICV and skull length measurements followed a very similar pattern, with a sharp
187 increase from P3 to P20 and then a plateau. In fact, the majority of bone deposition at the
188 cranial sutures occurs by P20. However, while none of the sutures fully fuse, except for

189 posterior frontal at about P10, most sutures narrow down to micrometer gaps at P20.
190 Nonetheless, intrinsic mechanical properties of the bone (approximately 4, 6 and 10 GPa at
191 P10, P20 and P70 respectively) and its thickness (approximately 30, 50 and 150 μm at P10,
192 P20 and P70 respectively) continue to increase (Moazen et al., 2015).

193

194 These data together highlight that, development of the brain, intracranial volume, intracranial
195 pressure and also perhaps bone mechanical properties are coupled. These changes occur
196 synchronously until the brain approximates adult size at P20, whereupon ICP and ICP
197 plateau, while bone elastic properties increasingly rigidify the skull (Moss, 1954). While the
198 data do not speak directly to the issue of whether ICP influences bone apposition at the
199 sutural margins (or is influenced by that apposition), they do suggest that the growth of the
200 neurocapsular matrix is not a response to overly high ICP, but rather that ICP rises when the
201 cranium slows its volumetric growth.

202

203 There were several limitations in this study. Firstly, it was not possible for us to visualize the
204 insertion of the needle into the skull, nor its final position. Therefore, we cannot be confident
205 that needle was in the subarachnoid space in all cases. However, an atlas of the developing
206 mouse (Aggrawal et al., 2009) was used to plan the needle insertion at various ages, and
207 the single operator (MM) was careful to insert the needle to the pre-identified depths to reach
208 the subarachnoid space. Secondly, animals were anesthetized using isoflurane, and this
209 might have had an impact on ICP (see e.g. Campkin, 1984; Scheller et al., 1987).

210 Nonetheless, the same procedure was applied to all animals, so the pattern of recorded ICP
211 in this study should remain valid. Finally, we cannot eliminate the possibility of a sex
212 difference in ICP because of missing data. However, at P31 there was no apparent effect of
213 sex.

214

215 In summary, this study quantified the changes in intracranial pressure during postnatal
216 development of the mouse. The results showed that ICP increases from about 1.3 mmHg at
217 P3 to 4 mmHg at P31, where it plateaus. These data can be used in computational models
218 of skull growth, allowing the strain patterns in the bone and sutures to be quantified.

219

220 **Conflict of interest**

221 The authors confirm that there is no conflict of interest in this manuscript.

222

223 **Acknowledgements**

224 This work was supported by the Royal Academy of Engineering Research Fellowship (MM)
225 and the Jean Renny Endowment for Craniofacial Medicine (MLC). We also thank Dr. Gerry
226 Hish for advice and assistance during this work.

227

228 **References:**

229 1. Al Dayeh, A.A., Rafferty, K.L., Egbert, M., Herring, S.W., 2013. Real-time monitoring
230 of the growth of the nasal septal cartilage and the nasofrontal suture. *Am J Orthod*
231 *Dentofacial Orthop.* 143(6), 773-783.

232

233 2. Aggarwal, M., Zhang, J., Miller, M.L., Sidman, R.L., Mori, S., 2009. Magnetic
234 resonance imaging and micro-computed tomography combined atlas of developing
235 and adult mouse brains for stereotaxic surgery. *Neuroscience.* 162(4),1339-1350.

236

237 3. Campkin, T.V., 1984. Isoflurane and cranial extradural pressure a study in
238 neurosurgical patients. *Br J Anaesth.* 56, 1083-1087.

239

- 240 4. Chuang, N., Mori, S., Yamamoto, A., Jiang, H., Ye, X., Xu, X., Richards,
241 L.J., Nathans, J., Miller, M.I., Toga, A.W., Sidman, R.L., Zhang, J., 2011. An MRI-
242 based atlas and database of the developing mouse brain. *Neuroimage*. 54(1), 80-89.
243
- 244 5. Cohen, M.M. 1993. Sutural biology and the correlates of craniosynostosis. *Am. J.*
245 *Med. Genet.* 47, 581-616.
246
- 247 6. Cox, T.C., Luquetti, D.V., Cunningham, M.L., 2013. Perspectives and challenges in
248 advancing research into craniofacial anomalies. *Am. J. Med. Genet. C Semin. Med.*
249 *Genet.* 163C:213-217.
250
- 251 7. Feiler, S., Friedrich, B., Schöller, K., Thal, S.C., Plesnila, N., 2010. Standardized
252 induction of subarachnoid hemorrhage in mice by intracranial pressure monitoring.
253 *J.Neurosci. Methods.* 190(2), 164-170.
254
- 255 8. Flurkey, K., Curren, J.M., Harrison, D.E., 2007. Mouse models in aging research. In:
256 Fox, J.G., et al. (Eds.), *The mouse in biomedical research-Volume 3 normative*
257 *biology, husbandry, and models.* Academic Press, Burlington MA., pp. 637-670.
258
- 259 9. Fong, K.D., Warren S.M., Loba, E.G., Henderson, J.H., Fang, T.D., Cowan, C.M.,
260 Carter, D.R., Longaker, M.T., 2003. Mechanical strain affects dura mater biological
261 processes: implications for immature calvarial healing. *Plast. Reconstr. Surg.* 112(5),
262 1312-1327.
263
- 264 10. Henderson, J.H., Nacamuli, R.P., Zhao, B., Longaker, M.T., Carter, D.R., 2005. Age-
265 dependent residual tensile strains are present in the dura mater of rats. *J R Soc*
266 *Interface* 2(3), 159-167.

267
268
269
270
271
272
273
274
275
276
277
278
279
280
281
282
283
284
285
286
287
288
289
290
291
292

11. Herring, S.W.,2008. Mechanical influences on suture development and patency. *Front. Oral. Biol.* 12, 41–56.

12. Hill, J.M., Lim, M.A., Stone M.M., 2008. Developmental milestones in the newborn mouse. In: Gozes I (Ed), *Neuropeptide techniques*. Humana Press Inc., Totowa NJ., pp.131-149.

13. Jones, H.C., Deane, R., Bucknall, R.M, 1987. Developmental changes in cerebrospinal fluid pressure and resistance to absorption in rats. *Brain Res.* 430(1), 23-30.

14. Moazen, M., Peskett, E., Babbs, C., Pauws, E., Fagan, M.J., 2015. Mechanical properties of calvarial bones in a mouse model for craniosynostosis. *PloS One.* 10(5), e0125757.

15. Mooney, M.P., Siegel, M.I., Burrows, A.M., Smith, T.D., Losken, H.W., Dechant, J., Cooper, G., Fellows-Mayle, W., Kapucu, M.R., Kapucu, L.O., 1998. A rabbit model of human familial, nonsyndromic unicoronal suture synostosis. II. Intracranial contents, intracranial volume, and intracranial pressure. *Childs Nerv Syst.* 14(6), 247-255.

16. Morriss-Kay, G.M., Wilkie, A.O.M., 2005. Growth of the normal skull vault and its alteration in craniosynostosis : insights from human genetics and experimental studies. *J. Anat.* 207, 637–653.

- 293 17. Moss, M.L., 1954. Growth of the calvaria in the rat: the determination of osseous
294 morphology. *Am. J. Anat.* 94,333-361.
295
- 296 18. Murtha. L., McLeod, D., Spratt, N., 2012. Epidural intracranial pressure measurement
297 in rats using a fiber-optic pressure transducer. *J. Vis. Exp.* 62. pii: 3689.
298
- 299 19. Nakata, S., 1981. Relationship between the development and growth of cranial
300 bones and masticatory muscles in postnatal mice. *J. Dent. Res.* 60(8), 1440-1450.
301
- 302 20. Opperman, L.A., 2000. Cranial Sutures as intramembranous bone growth sites.
303 *Dev.Dyn.*485, 472–485.
304
- 305 21. Oshio, K., Watanabe, H., Song, Y., Verkman, A.S., Manley, G.T., 2005. Reduced
306 cerebrospinal fluid production and intracranial pressure in mice lacking choroid
307 plexus water channel Aquaporin-1. *FASEB J.* 19(1), 76-8.
308
- 309 22. Raboel, P.H., Bartek, Jr. J., Andresen, M., Bellander, B.M., Romner, B., 2012.
310 Intracranial pressure monitoring: invasive versus non-invasive methods - a review.
311 *Crit. Care Res. Pract.* 950393: 14 pages.
312
- 313 23. Richtsmeier, J.T., Flaherty, K., 2013. Hand in glove: brain and skull in development
314 and dysmorphogenesis. *Acta Neuropathol.* 125(4), 469-489.
315
- 316 24. Rafferty, K.L., Herring, S.W., 1999. Craniofacial sutures: morphology, growth and in
317 vivo masticatory strains. *J Morph.* 242,167-179.
318

- 319 25. Scheller, M.S., Todd, M.M., Drummond, J.C., Zornow, M.H., 1987. The intracranial
320 pressure effects of isoflurane and halothane administered following cryogenic brain
321 injury in rabbits. *Anesthesiology*. 67, 507-512.
322
- 323 26. Silasi, G., MacLellan, C.L., Colbourne, F., 2009. Use of telemetry blood pressure
324 transmitters to measure intracranial pressure (ICP) in freely moving rats. *Curr*
325 *Neurovasc Res*. 6(1), 62-69.
326
- 327 27. Uldall, M., Juhler, M., Skjolding, A.D., Kruuse, C., Jansen-Olesen, I., Jensen, R.,
328 2014. A novel method for long-term monitoring of intracranial pressure in rats. *J.*
329 *Neurosci. Methods*. 227, 1-9.
330
- 331 28. Yang, B., Zador, Z., Verkman, A.S., 2008. Glial cell aquaporin-4 overexpression in
332 transgenic mice accelerates cytotoxic brain swelling. *J. Biol. Chem*. 283(22), 15280-
333 15286.
334
- 335 29. Zhang, J., Miller, M.I., Plachez, C., Richards, L.J., Yarowsky, P., van Zijl, P., Mori, S.,
336 2005. Mapping postnatal mouse brain development with diffusion tensor
337 microimaging. *NeuroImage*. 26, 1042-1051.
338

339 **Figures legend**

340

341 **Fig 1:** (A) Testing of the pressure sensor with varying heights of water. The needle was
342 slowly inserted to the bottom of a tube of water, held there for 10-25 sec, and then slowly
343 removed. (B) Calibration of the pressure sensor showed the response was linear. Small
344 brackets indicate the SD of measurements.

345

346 **Fig 2:** Changes in intracranial pressure during wild type mouse development (means and
347 SDs). The shaded areas indicate ICP data for all samples in the corresponding age group.
348 Asterisks show statistically significant differences.

349

350 **Fig 3:** (A) A P70 mouse, highlighting the sagittal and coronal planes used for length and
351 width comparisons. (B) Sagittal and (C) coronal sections of one animal per age. Note the
352 P10 skull became slightly deformed following the ICP measurement and prior to micro-CT
353 scanning. (D) Skull length, width and (E) intracranial volume at P3, P10, P20, P31 and P70.

354

355

356

357

358

359

360

361

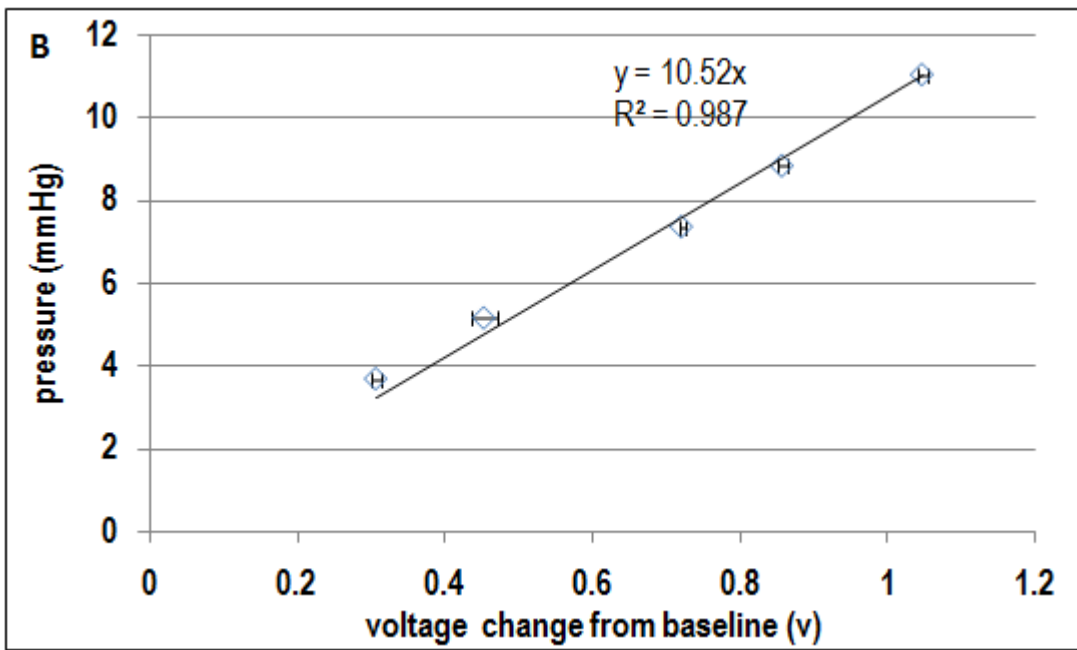
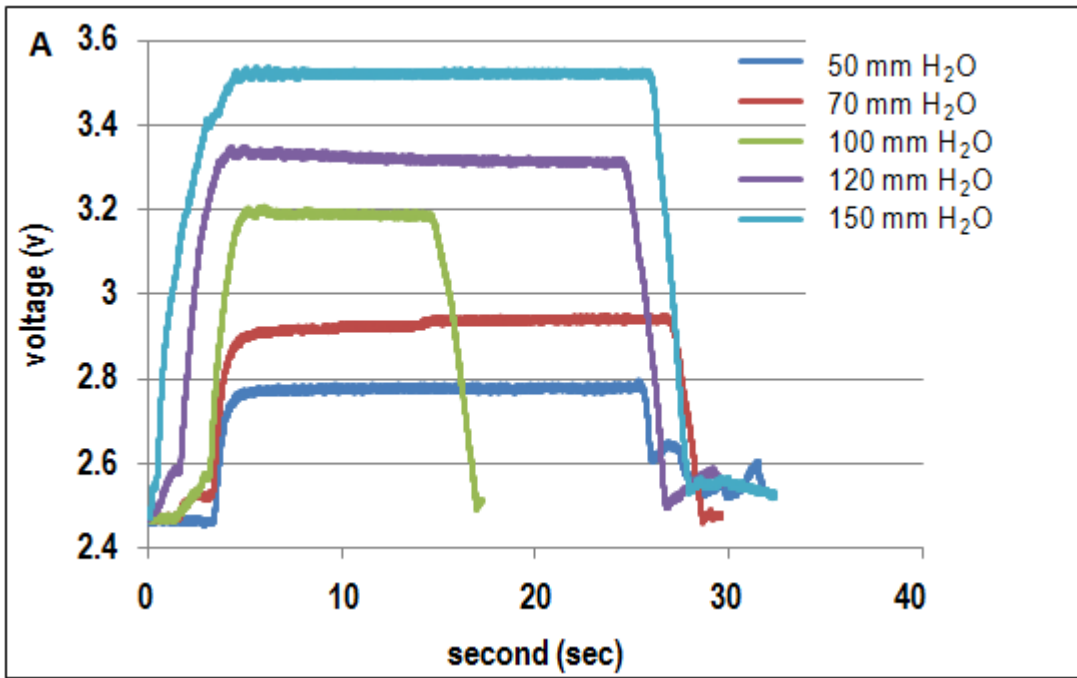
362

363

364

365

366 Fig 1



367

368

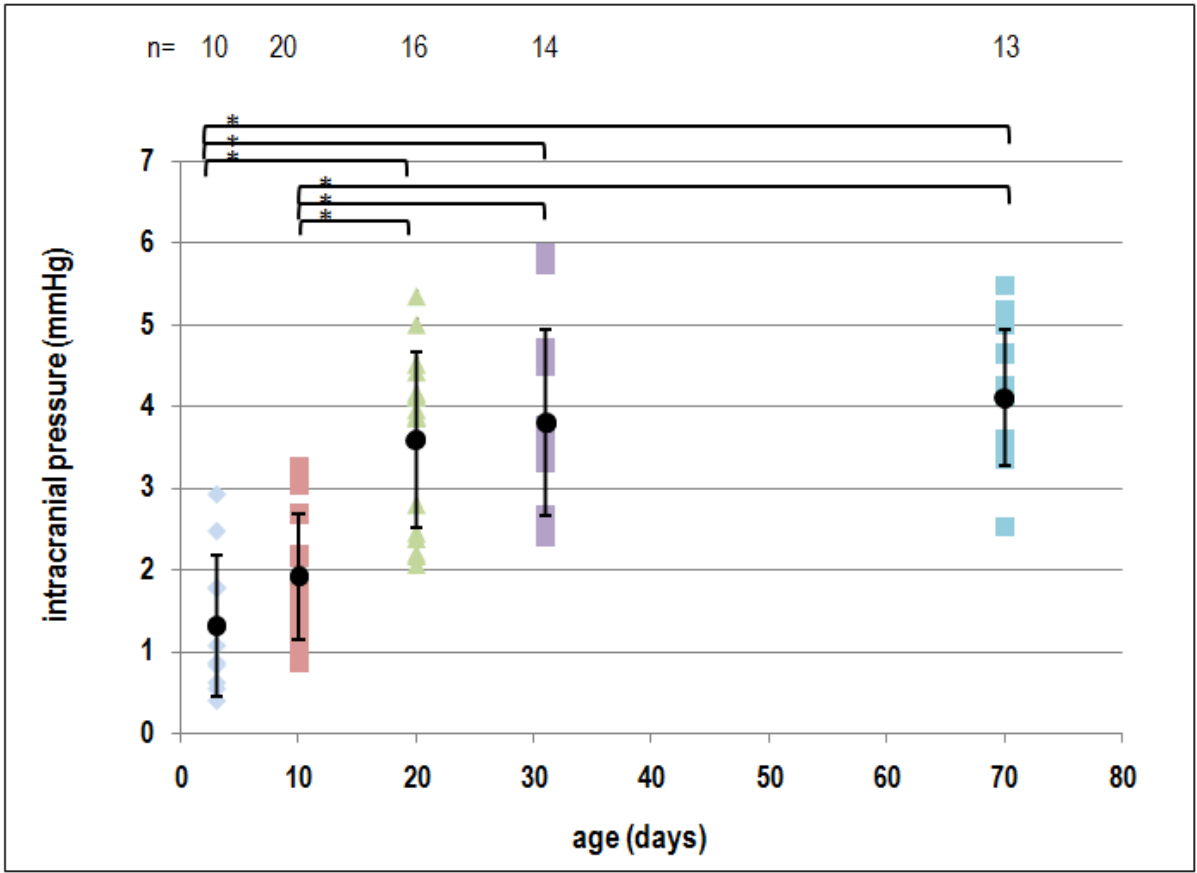
369

370

371

372

373 Fig 2



374

375

376

377

378

379

380

381

382

383

384

385

386

